Micro-Brownian Motion of Polymer Segments in a Monolayer at the Air−Water Interface: A Time-Resolved Study of Intralayer Energy Transfer

Shinzaburo Ito, Satoshi Oki, Nobuhiro Sato, and Masahide Yamamoto*

Division of Polymer Chemistry, Graduate School of Engineering, Kyoto University, Sakyo, Kyoto 606-01, Japan

Received September 16, 1994; Revised Manuscript Received May 13, 1995[⊗]

ABSTRACT: This work is concerned with micro-Brownian motion of polymer segments on a water surface, which is observed as the lateral diffusion of fluorescence probes attached to the polymer chains. Poly(vinyl octanal acetal)s labeled with phenanthrene (P: energy donor) and anthracene (A: energy acceptor) are spread on water, yielding a stable monolayer in which the probes are able to take statistically random distributions in the two-dimensional plane. The time-resolved fluorescence analysis of the energy transfer between the P and A probes allows us to evaluate the acceptor densities and lateral diffusion coefficients of polymer segments on the water surface. The result is obtained by fitting the fluorescence decay data with the theoretical prediction by the Monte Carlo simulation. It is found that this polymer forms a viscous monolayer, in which the lateral diffusion of polymer segments takes place with a diffusion coefficient of ca. 8×10^{-8} cm^2 s^{-1}.

Introduction

Since the Langmuir−Blodgett (LB) technique is capable of controlling spatial arrangement of organic molecules with a molecular dimension, extensive studies on LB films have been made aiming to explore and construct functional thin films.[1] From a standpoint of preparing thin organic films, preformed polymer LB films, which are made by transferring a polymer monolayer onto a solid substrate, have the potential to overcome some drawbacks of conventional fatty acid LB films.[2,3] An excellent review written by Crisp 40 years ago provides detailed information about the phase behavior of polymer monolayers mainly from the surface pressure−area isotherms.[4] However, we have little knowledge about fundamental properties of the polymer monolayer, especially the dynamic behavior of a monolayer on a water surface. The dynamic characters as well as the static morphology of the monolayer are crucial to the fabrication of polymer LB films with high quality. These issues also draw much scientific interest in relation to polymer chemistry and physics for systems confined in a two-dimensional plane.

There have been a couple of attempts to elucidate the dynamic behavior of a surface monolayer. Meller et al. have studied lateral diffusion in monolayers of polymerizable amphiphiles.[5] They employed the FRAP (fluorescence recovery after photobleaching) technique. Fluorescence dyes incorporated into a monolayer were bleached by laser light under a fluorescence microscope, and they observed the recovery of fluorescence intensity due to lateral diffusion of dyes from the unbleached region. Monitoring the rate of recovery, they could obtain the diffusion constants for various amphiphilic lipid monolayers. Most of lipids showed values in the order of 10^{-7} cm^2 s^{-1}, but the rate of diffusion rapidly decreased as polymerization proceeded on the water surface. Yu et al. have applied this FRAP method to various monolayer systems.[6] One of samples they employed was a vinyl polymer, poly(*tert*-butyl methacrylate) (PBMA) which forms an expanded type monolayer. The diffusion constants obtained for the liquid-phase were on the order of 10^{-8} cm^2 s^{-1} and dropped to zero (below the limit experimentally detectable) with compression of monolayer to the limiting area of monomer unit: 0.28 nm^2.

Another approach using the fluorescence technique has been performed by Caruso et al.[7] They observed the quenching phenomenon of pyrene fluorescence as a function of quencher concentrations; both types of probes were mixed in the amphiphilic monolayer. The theoretical analysis provided diffusion constants of these probes in the monolayer, being ca. 10^{-7} cm^2 s^{-1}. These experiments indicate that the fluorescence technique is quite useful for probing lateral diffusion of monolayers because of the high sensitivity of fluorescence detection.

In the current paper, we demonstrate another fluorescence method to evaluate lateral diffusion constants in a monolayer on a water surface. Both energy-donating and -accepting probes are covalently bonded to a polymer chain, poly(vinyl octanal acetal), which is known to form a stable monolayer on water/air interface, and can also be nicely deposited onto various substrates.[8,9] The enhanced energy transfer caused by mutual diffusion of donor and acceptors is directly measured at the air/water interface by the time-resolved fluorescence apparatus. Since the probes are attached to the polymer chains, the values obtained can be regarded as the diffusion constants of polymer segments in the monolayer. We think that this is first report to elucidate the mobility of polymer segments in the monolayer spread at the gas−liquid interface.

Experimental Section

Materials. Poly(vinyl octanal acetal) (PVO) labeled with fluorescent chromophores were synthesized by acetalization of commercial poly(vinyl alcohol) (PVA, Wako Chemicals, atactic with a racemic content of 0.55, dp = 2000 on average of polydispersity) with octanal and chromophoric aldehydes. The procedures have been described elsewhere.[10] The chemical structures of the resulting polymers are shown in Figure 1. The acetal rings of PVO are produced mainly at the isotactic sequence of PVA, because of the larger reactivity compared with the syndiotactic sequence. In addition to the nonlabeled PVO, we prepared two kinds of PVO's, one of which contains only phenanthrene (P) chromophore as a control sample of donor emission, and the other contains both P and anthracene

[⊗] Abstract published in *Advance ACS Abstracts,* December 1, 1995.

0024-9297/96/2229-0724$12.00/0

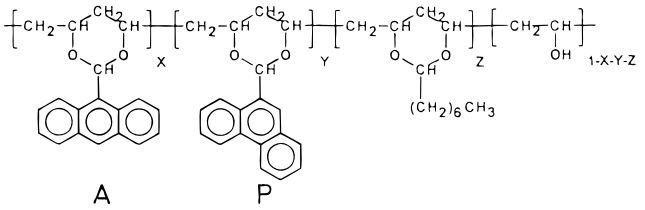

Figure 1. Molecular structures of chromophoric poly(vinyl octanal acetal)s.

Table 1. Compositions of Synthesized Polymers[a]

sample	X, %	Y, %	Z, %
PVO-P	0	12	57
PVO-PA	0.43	5.7	63

[a] For definitions of X, Y, Z, see Figure 1.

(A) as a pair of energy donor and acceptor moieties. These are hereinafter abbreviated as PVO-P and PVO-PA, respectively. Table 1 shows the compositions of these polymers, in which the contents of octanal units and chromophoric units were determined from the UV absorption spectra and the elemental analysis.

Preparation of Monolayer. A dilute solution of PVO in benzene (Dojin Spectrograde) was spread onto pure water in a Teflon-coated trough (Kenkosha model SI-2) equipped with a Wilhelmy-type film balance. The water was purified by distillation and then passed through a water purification system (Barnstead nanopure II).

Measurements. The details of the apparatus used in this study have been described elsewhere.[11] We employed a pair of quartz optical fibers 3 mm in diameter. One was used as a light guide for excitation and its one end was positioned in the middle of trough at a distance of 5 mm above the water surface and at an angle of 45° by the surface plane. The other end of this fiber was connected to an excitation light source, which is either a xenon lamp for the steady state excitation or a mode-locked argon synchronously pumped dye laser system with a frequency doubler (Spectra Physics) for the case of time-resolved measurements. The other fiber was used as a light guide for observing fluorescence from the surface film, which was arranged just above the illuminated area at a right angle to the surface plane. The detecting fiber was introduced into a fluorescence spectrometer (Hitachi model 850) or to a time-correlated single photon counting system. The total response time of the time-resolved instrument was 600 ps for the full width at half maximum (FWHM) of the excitation pulse. To remove oxygen quenching, nitrogen gas was gently passed over the water surface.

The morphology of surface film was observed by a Brewster angle microscope (BAM)[12,13] which was built in our laboratory using a He-Ne laser (Uniphase model 1135P, 10 mW) and a CCD camera (Hitachi model KP-M1) equipped with a camera controller (Hamamatsu C2400).

Results and Discussion

Steady State Spectroscopy. It is known that PVO forms a stable, condensed-type monolayer on a water surface.[8] The collapse pressure at 20 °C is around 25−30 mN m^{-1}, depending on the content of the alkyl units and the fraction of chromophoric units. Previous works showed that the presence of chromophore up to 15% did not affect the stability of the monolayer, which could be transferred onto solid substrates with a good transfer ratio around unity, although a gradual decrease of the collapse pressure was observed with the increase of chromophore content.[14,15]

Figure 2 shows the fluorescence spectrum of PVO-PA monolayer at 20 mN m^{-1}. The P units are selectively excited by 290 nm light through an interference filter with a band width of 10 nm. The emission from the monolayer is so weak that we have to choose a wide

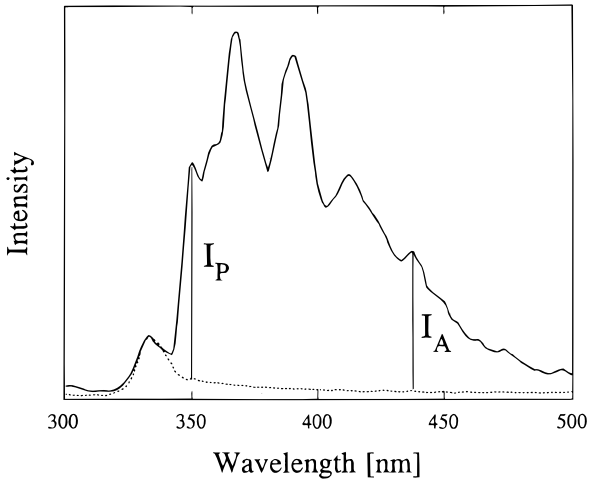

Figure 2. Fluorescence spectrum of PVO-PA monolayer at 20 mN m^{-1} on a water surface at 18 °C. The dotted line shows the background signal without the monolayer, mainly due to the Raman scattering of water. Excitation: 290 nm, band width 10 nm, and the emission band width: 3 nm.

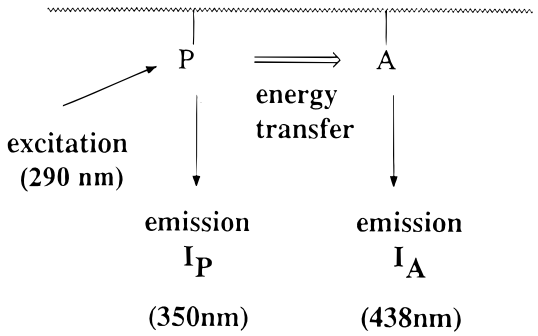

Figure 3. Scheme of excitation and energy transfer processes.

aperture of the monochrometor and this results in a broader spectral resolution: 3 nm. The solid line of Figure 2 shows the donor P fluorescence at 350−370 nm and the acceptor A fluorescence in the longer wavelength range of 390−450 nm; the A emission is enhanced by the energy transfer from the excited P. Under the same conditions, we have rather strong Raman scattering of water around 330−340 nm which cannot be avoided in the observation of water surface. Although there are some difficulties due to the weak intensity of fluorescence from the monolayer, the emission spectrum can be observed with sufficient sensitivity even for the monolayer containing only a few percent of chromophores. Figure 2 clearly demonstrates that efficient intralayer energy transfer takes place in the PVO-PA monolayer, according to the scheme drawn in Figure 3. As a convenient measure of energy transfer efficiency, we employed the fluorescence intensity ratio, I_A/I_P, where I_A is the fluorescence intensity of A unit at 438 nm and I_P is that of P at 350 nm. The larger I_A/I_P means the higher efficiency of intralayer energy transfer.

Figure 4 depicts the intensity ratio as a function of surface concentration. The broken line in this figure shows the surface pressure plotted against the surface concentration. When the monolayer is compressed from the expanded state, one can see gradual increase of the energy transfer efficiency as expected, because of the closer distance of separation between P and A moieties. There is no drastic change in the range of dilute concentrations below the critical concentration c^* at which the surface pressure begins to rise steeply. A

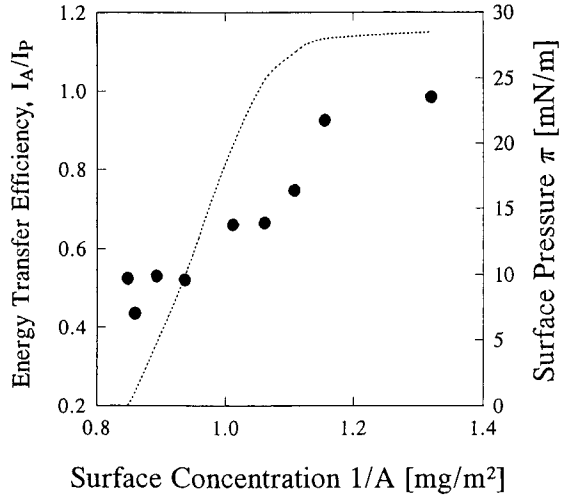

Figure 4. Energy transfer efficiencies as a function of surface concentration. The dotted line shows the surface pressure at 18 °C.

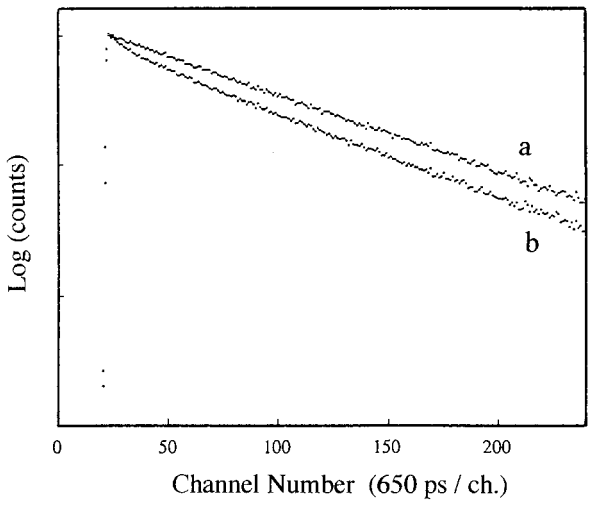

Figure 5. Fluorescence decay curves observed at 370 nm for (a) PVO-P and (b) PVO-PA at 15 mN m^{-1}, 18 °C.

BAM study revealed that the surface film forms a so-called island structure in the dilute range, i.e., a large domain of the monolayer is floating on a part of the water surface. Therefore the photophysical processes in a domain seem to be independent of the macroscopic surface pressure when it is lower than c^*. At concentrations higher than the collapse pressure, the transfer efficiency still increases with compression. This may result from interlayer energy transfer owing to the folded film structure. From now on, our discussion should be focussed on the fluorescence behavior in the middle range of Figure 4 where the surface pressure is detectable, but below the collapse pressure of this monolayer.

Time-Resolved Fluorescence Spectroscopy. A pulsed laser beam at 298 nm was used to illuminate the water surface and selectively excite the donor P in the PVO monolayer. The resulting fluorescence decay curves were recorded by a single photon counting system through the optical fiber. Figure 5 shows the obtained decay curves of donor emission at 370 nm for both PVO-P and PVO-PA. Of course, the emission from PVO-P decreased with a single exponential function of time because no chromophore interaction between P and A occurred in this system. The lifetime of the excited P unit was evaluated to be 47 ns from the slope of the

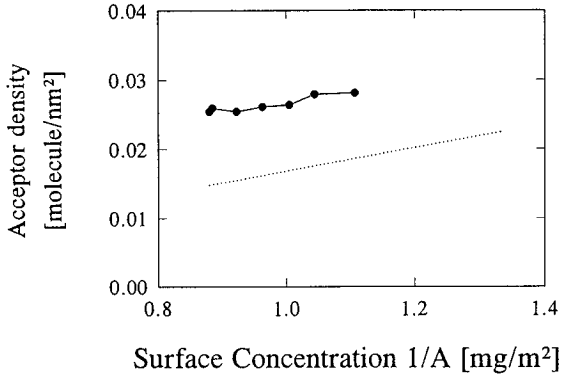

Figure 6. Surface acceptor densities (●) obtained by the decay analysis using the Hauser equation. The dotted line shows the densities of the acceptor calculated by the polymer composition, the amount of polymer spread on the surface, and the surface area.

decay curve in the semilogarithmic plot. Contrary to this, the PVO-PA monolayer gave rise to a faster decay which could not be fitted with an exponential function. Obviously there is an additional deactivation process, namely, energy transfer from the excited P to A units. At first we tried to fit the decay data with a theoretical decay function given by a two-dimensional Förster mechanism. Hauser et al. derived the theoretical equation:[16]

$$I(t) = \exp\{-t/\tau_0 - 2g(t/\tau_0)^{1/3}\} \quad (1)$$

where

$$g = {}^2/_3 n_A \pi R_0^2 \quad (2)$$

and τ_0 is the intrinsic lifetime of the excited donor P without A, n_A is the number of acceptors in a unit area, and R_0 is the Förster radius given by spectral overlap of the absorption spectrum of A and the fluorescence spectrum of P, being estimated to be 2.24 nm for the present donor and acceptor pair. This equation is applicable to the energy transfer caused by the dipole−dipole interaction between a donor and an acceptor distributed randomly in a two-dimensional plane. Judging from the residual plots and the mean square residuals, χ^2, we got a good fit with eq 1 ($\chi^2 < 1.4$), providing the value of parameter g which contains the acceptor density n_A on the water surface. The densities evaluated from the best fit are plotted against the surface concentration of the polymer in Figure 6. It looks very reasonable that the density linearly increases with the increase of polymer concentration. However, the obtained values are stoichiometrically unacceptable; the density could be calculated from the weight of polymer spread on the water surface and from the content of acceptors in the polymer chain which has been already determined by UV absorbance and elemental analysis. The calculated values are drawn by the dotted line in Figure 6, showing that the experimental data obtained by the decay analysis are about twice that of the real surface densities.

To solve this discrepancy, we have to take into account lateral diffusion of the polymer segments on the water surface. During the lifetime of excited P, both P and A, which are covalently linked to polymer chains, can move and approach each other, resulting in a higher energy transfer efficiency compared with the frozen model mentioned above. Theoretical consideration for

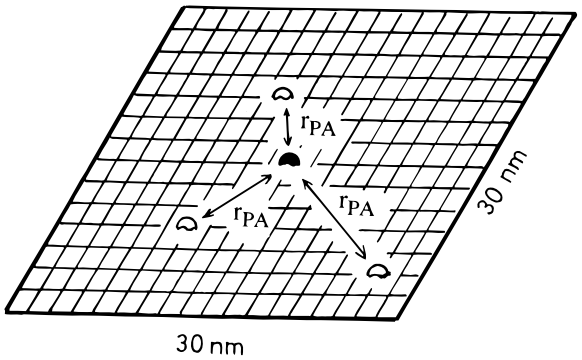

Figure 7. Schematic illustration of the two-dimensional model used for Monte Carlo simulation.

the Förster energy transfer in three-dimensional systems has been performed by many workers. As to the extreme case that the translational diffusion of molecules is strictly restricted ($D = 0$), the Förster equation has been applied and widely accepted.[17] Another extreme case, where the diffusion is so fast that one can neglect the gradient of the transfer rate on the distance of separation ($D \gg R_0^2/\tau_0$), can be represented by the well-known Smoluchowski equation involving a step function of reaction probability at an encounter radius of reaction.[18] It is, however, quite difficult to express the intermediate system by an analytical equation. Currently, the Yokota−Tanimoto Pade model has been utilized to the energy transfer system involving mutual diffusion of donor and acceptors.[19] Our interest is now pointing toward the two-dimensional intermediate system, but there is no appropriate equation for this intermediate system, although equations for both the extreme cases of two-dimensional diffusion have already been reported by Hauser[16] and Owen.[20] Therefore we employed a numerical method which is applicable to a wide range of configurations of donor−acceptor systems.[21,22]

As illustrated schematically in Figure 7, a donor P is placed at the center of a square plane, and acceptors A's are distributed statistically according to a given surface concentration. The energy transfer rate from the donor i to all acceptors is calculated by eq 3,

$$k_{Ti} = (1/\tau_0)\sum_j (R_0/r_{ij})^6 \tag{3}$$

where r_{ij} is the distance between donor i and acceptor j. If the molecules are fixed at the given positions during the donor lifetime, the decay curve of the donor is simply given by eq 4,

$$I_i(t) = \exp(-t/\tau_0 - k_{Ti}t) \tag{4}$$

and the average of eq 4 for many patterns of the acceptor distributions is able to reproduce eq 1.

In the present system, the movement of molecules alters the distance r_{ij} with time, therefore, k_{Ti} is now time-dependent in eq 4. In order to obtain $I_i(t)$ by the numerical calculation including this movement, let us consider a small step of movement Δd, 0.05 nm, whose direction on the plane is determined by a random number produced by a computer. After a short time interval $dt = 0.5$ ns, the location and mutual distances of the donor and acceptors are recalculated, and then the rate k_{Ti} at a given time is determined by eq 3. This procedure is repeated over the whole time range of observation, 250 ns. Using eq 4 and k_{Ti} at each time interval, one can get the decay curve of the donor i.

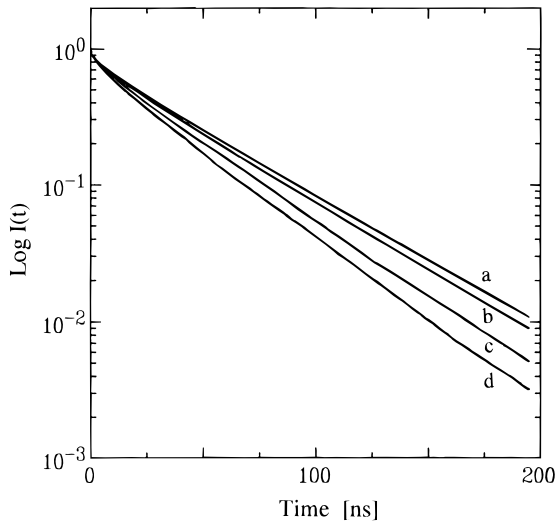

Figure 8. Calculated donor fluorescence decay curves for various diffusion constants. $D =$ (a): 0, (b): 1×10^{-7} cm^2 s^{-1}, (c) 5×10^{-7} cm^2 s^{-1}, and (d) 1×10^{-6} cm^2 s^{-1}.

Finally, the average for n_P donors is obtained by

$$I(t) = (1/n_P)\sum_i I_i(t) \tag{5}$$

where n_P is employed as 500, which is large enough to reach the statistical convergence.

Figure 8 depicts some decay curves calculated for various values of diffusion constant D. Of course, the curve for $D = 0$ is exactly the same as that from eq 1, showing rapid decrease at the initial stage after the excitation and then slow decay with a slope close to the intrinsic lifetime τ_0. The feature is changed with the increase of D; the excitation energy on P has a possibility of energy transfer to some A's even in the later time range due to the displacement from the initial position. This results in the faster decay with smooth curvature of the decay curve compared with the case of $D = 0$. Now, it becomes possible to fit the experimental data to these calculated curves by the least-squares fitting method. This operation is repeated for various values of D to obtain the best value of D for fitting. Figure 9 demonstrates a few fitting results using one of the experimental data at 15 mN m^{-1}. The upper part of each figure shows the residual plots of decay curve which indicate the tendency of deviation depending on the magnitude of D values.

Figure 10 is a plot of the mean square of residuals as a function of D. From the minimum of residuals, the best fit value of D is found to be 8×10^{-8} cm^2 s^{-1}, and the mean displacement L during the lifetime of the donor, 47 ns, is evaluated to be 1.3 nm, using the following equation.

$$L = (4D\tau_0)^{1/2} \tag{6}$$

Taking into account the molecular dimension of an acetal unit, 0.6 nm, being obtained from the limiting area of the surface pressure−area isotherm, it can be said that the polymer segments are able to move around two units during the lifetime. These results indicate that the polymer monolayer maintains its mobility even in the liquid-condensed phase, although the mobility is as small as that in polymer melt or concentrated solutions in three-dimensional systems.

Finally, it should be noted that the energy transfer method is often accompanied with an uncertainty aris-

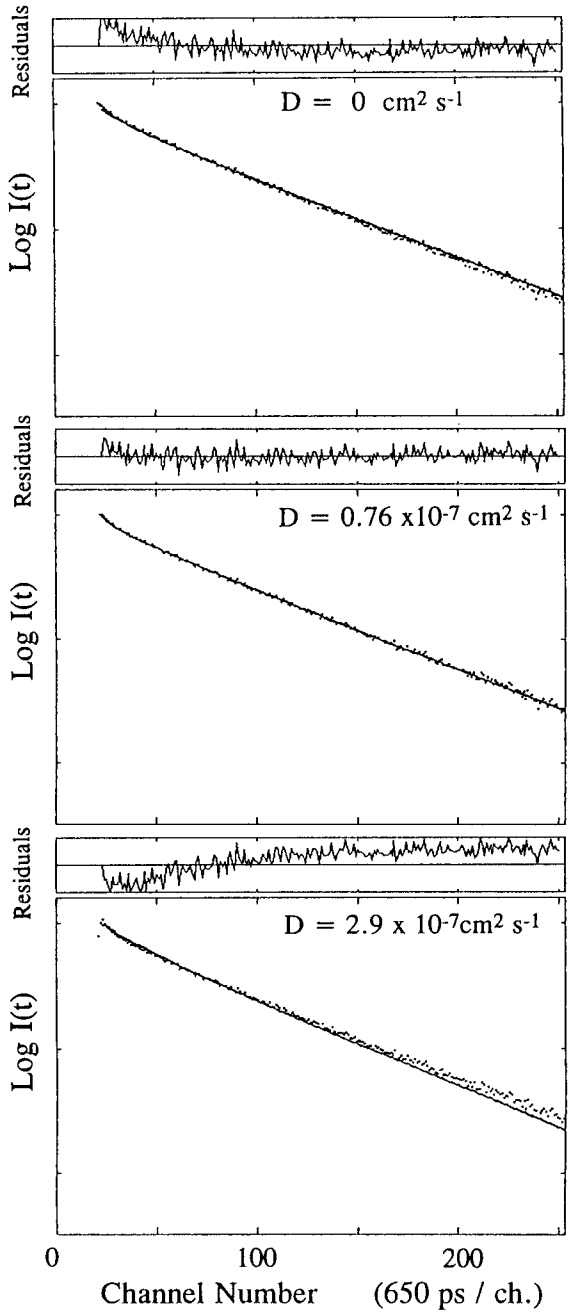

Figure 9. Fittings of the fluorescence decay for PVO-PA monolayer with calculated curves. The full scale of residual plot is ±10, defined as res = $(I(t) - F(t))/(F(t))^{1/2}$, where $F(t)$ is the fitting function and $I(t)$ is the experimental value.

ing from the orientation of chromophores. The formula of Förster radius R_0 contains the orientation factor k^2, which is ambiguous in many cases and may introduce a large error in evaluation of distances. Therefore, the value of k^2 has to be chosen under an appropriate model for the molecular orientation of donors and acceptors. Dale et al. reported detailed calculations of k^2 for various orientational models.[23] It is known that $k^2 = 0.667$ when the molecules take a random orientation and rotate rapidly during the donor lifetime. But, if the chromophoric units take a preferential orientation due to some specific interaction between hydrophilic units and water, the transition moments of the donor and acceptors may be inclined at a given angle to the water surface. In this case, the transition moments are restricted to the surface of a cone whose axis is normal to the water surface. Tweet et al. derived the following

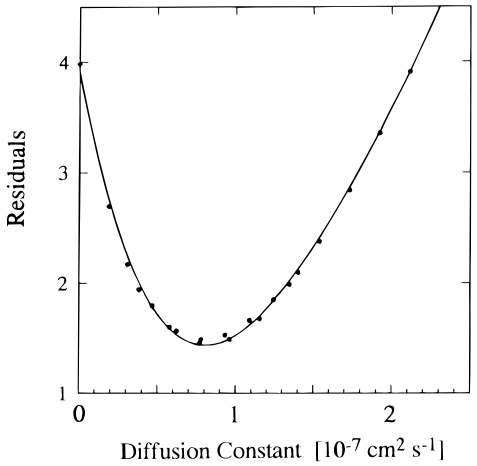

Figure 10. Residual plots as a function of diffusion constants.

equation,[24]

$$k^2 = \cos^4 \delta + {}^5/_4 \sin^4 \delta \qquad (7)$$

where δ is the half-cone angle, i.e., the tilt angle from the cone axis. This equation tells us that the minimum of k^2 is 0.555 at $\delta = 42°$ and the maximum 1.25 comes out at $\delta = 90°$. In the latter case, all transition moments lie on the water surface and take all azimuths about the normal to the water surface. Thus, under this assumption, the value of R_0 is altered in the range of 2.17−2.48 nm, as a function of the angle δ.

In the present study, we employed 2.24 nm for R_0 using $k^2 = 0.667$, which is the value for the random distribution of transition moments. The reasons we did not use the cone model are as follows. At first, the transition moment of donor P cannot be regarded as a linear dipole because the intrinsic polarization of P fluorescence is very low. If the transition moment is purely a linear dipole, the emission from randomly oriented dipoles in the frozen state would show a high fluorescence anisotropy around 0.4 when excited with linearly polarized light.[25] However, the anisotropy actually observed for P in solid matrices is only 0.05 (P chromophores were randomly embedded in a cast film). This indicates that even if the molecules are aligned to a certain angle to the water surface, the transition moments, especially of the donor P, are intramolecularly randomized due to their own electronic character. Secondly, the polymer structure provides rotational freedom to the chromophoric units and configurational variation to the acetal rings. These polymers are prepared from atactic PVA, the isotactic and syndiotactic diads yielding different types of acetals with respect to the substitution to the main chain. It is hard to consider a preferential orientation for both of tactic sites. Thirdly, the monolayer maintains its mobility, which was also confirmed by a study of pyrene-labeled PVO monolayer in terms of the dynamic behavior of excimer formation. Taking into account these facts, it is more reasonable to employ the randomized model than the strictly restricted cone model. Finally it should be noted that the variation of $R_0 = 2.48-2.17$ nm predicted by eq 7 results in alteration of D in the range of 3×10^{-8} to 1×10^{-7} cm^2 s^{-1}.

Conclusion

Lateral diffusion coefficients of polymer segments in a PVO monolayer on a water surface were determined

by the energy transfer method. The fluorescent probes were covalently and randomly attached to the polymer chains. Therefore, the monolayer could provide a statistically random distribution of probes in the two-dimensional plane. This enabled us to apply a theoretical calculation using the Monte Carlo method and to fit the fluorescence decay with the simulation curves. The diffusion coefficient obtained was on the order of 10^{-8} cm^2 s^{-1}, which is similar to the values reported by the FRAP technique for a PBMA monolayer in the expanded region.[5] But, PBMA showed strong dependence of D on the applied surface pressure, and the D became nearly zero in the liquid-condensed state, whereas the PVO monolayer still kept the mobility at higher pressures. One explanation for this difference is that this mobility is due to micro-Brownian motion of polymer segments on a nanometer scale, which may differ from macroscopic lateral diffusion of monolayer observed by the FRAP method. Such a viscous but mobile character in the molecular dimension could be one of the reasons for the excellent deposition of PVO onto various substrates in the preparation of LB films from the water surface.

Acknowledgment. This work is in part supported by a Grant-in-Aid for Scientific Research (No. 06651050) from the Ministry of Education, Science and Culture of Japan.

References and Notes

(1) Kuhn, H.; Möbius, D.; Bücher, H. In *Physical Methods of Chemistry*; Weissberger, A., Rossiter, B. W., Ed.; Wiley: New York, 1972; Vol. 1, Part 3B, p 577.
(2) Tredgold, R. H. *Thin Solid Films* **1987**, *152*, 223.
(3) Wegner, G. *Thin Solid Films* **1992**, *216*, 105.
(4) Crisp, D. In *Surface Phenomena in Chemistry and Biology*; Danielli, J. F., Pankhurst, K. G. A., Riddiford, A. C., Eds.; Pergamon: London, 1958; p 23.
(5) Meller, P.; Peters, R.; Ringsdorf, H. *Colloid Polym. Sci.* **1989**, *267*, 97.
(6) (a) Kim, S.; Yu, H. *J. Phys. Chem.* **1992**, *96*, 4034. (b) Tamada, K.; Kim, S.; Yu, H. *Langmuir* **1993**, *9*, 1545.
(7) (a) Caruso, F.; Grieser, F.; Murphy, A.; Thistlethwaite, P.; Urquhart, R.; Almgren, M.; Wistus, E. *J. Am. Chem. Soc.* **1991**, *113*, 4838. (b) Caruso, F.; Grieser, F.; Thistlethwaite, P. J.; Almgren, M. *Langmuir* **1993**, *9*, 3142. (c) Caruso, F.; Grieser, F.; Thistlethwaite, P. J.; Furlong, D. N. *Macromolecules* **1994**, *27*, 77.
(8) Watanabe, M.; Kosaka, Y.; Oguchi, K.; Sanui, K.; Ogata, N. *Macromolecules* **1988**, *21*, 2997.
(9) Ohmori, S.; Ito, S.; Yamamoto, M.; Yonezawa, Y.; Hada, H. *J. Chem. Soc., Chem. Commun.* **1989**, 1293.
(10) Ohmori, S.; Ito, S.; Yamamoto, M. *Macromolecules* **1990**, *23*, 4047.
(11) Ito, S.; Oki, S.; Hayashi, T.; Yamamoto, M. *Thin Solid Films* **1994**, *244*, 1073.
(12) Henon, S.; Meunier, J. *Rev. Sci. Instrum.* **1991**, *62*, 936.
(13) Hönig, D.; Möbius, D. *J. Phys. Chem.* **1991**, *95*, 4590.
(14) Ito, S.; Okubo, H.; Ohmori, S.; Yamamoto, M. *Thin Solid Films* **1989**, *179*, 445.
(15) Ohmori, S.; Ito, S.; Yamamoto, M. *Macromolecules* **1991**, *24*, 2377.
(16) Hauser, M.; Klein, U. K. A.; Gösele, U. *Z. Phys. Chem., NF* **1976**, *101*, 255.
(17) Förster, Th. *Ann. Phys.* **1948**, *2*, 55.
(18) Smoluchowski, M. *Z. Phys. Chem.* **1917**, *92*, 129.
(19) Yokota, M.; Tanimoto, O. *J. Phys. Soc. Jpn.* **1967**, *22*, 779.
(20) Owen, C. S. *J. Chem. Phys.* **1975**, *62*, 3204.
(21) Hayashi, T.; Okuyama, T.; Ito, S.; Yamamoto, M. *Macromolecules* **1994**, *27*, 2270.
(22) Yamamoto, M.; Kawano, K.; Okuyama, T.; Hayashi, T.; Ito, S. *Proc. Jpn. Acad., Ser B* **1994**, *70*, 121.
(23) Dale, R. E.; Eisinger, J. In *Biochemical Fluorescence: Concepts*; Chen, R. F., Edelhoch, H., Eds.; Marcel Dekker: New York, 1975; p 115.
(24) Tweet, A. G.; Bellamy, W. D.; Gaines, G. L. *J. Chem. Phys.* **1964**, *41*, 2068.
(25) Wahl, P. In the same book as ref 23, chap. 1.

MA9464276